A chloride conductance exhibiting bicarbonate conductivity in renal inner medullary collecting duct cells

Juan J. Bolívar, César O. Lara-Figueroa, Ramón H. Martínez-Mayorquin, Florencio Monroy-Romero and Gabina Arenas

Department of Physiology, Faculty of Medicine, National Autonomous University of Mexico, Mexico City, Mexico

Abstract. The anion conductance in primary cultures of rat inner medullary collecting duct cells was studied using perforated-patch whole-cell clamp technique. Depolarizations above 0 mV induced an outward anionic current with a time-dependent activation (I_{ovt}) exhibiting a similar conductivity to Cl^- and HCO_3^-. I_{ovt} showed half-maximal activation around 32 mV with a slope factor of 23 mV, and showed a voltage-dependent activation time course that was well fitted by a sum of two exponential functions. I_{ovt} was potentiated when external pH values or external Ca^{2+} concentration was increased and was blocked by external DIDS, DPC and furosemide. These characteristics of I_{ovt} resemble that of the ClC-K1 channels-mediated currents; however, anion substitution studies showed that I_{ovt} exhibits a $Br^- > Cl^- > I^- > NO_3^-$ conductivity sequence, different from that observed in the ClC-K1 channels-mediated conductance. We suggest that, in inner medullary collecting duct cells, ClC-K channels of an unidentified type give rise to this Cl^- and HCO_3^- conductance. This is the first study of a channel-mediated HCO_3^- current in kidney tubular cells.

Key words: Kidney — Anion channel — Bicarbonate transport — Cl^- current — IMCD

Introduction

Two decades ago, studies performed on rat and hamster perfused isolated inner medullary collecting ducts (IMCD) reported the presence of a bicarbonate conductance at the basolateral membrane of IMCD cells (Stanton 1989; Imai and Yoshitomi 1990). Neither any other anionic conductance at this membrane nor any anionic conductance at the apical membrane was observed in those studies. Since these earlier reports, some studies performed on IMCD cells in primary culture reported the presence of a cystic fibrosis transmembrane regulator (CFTR) chloride conductance and of a Ca^{2+}-activated chloride (CaC) conductance, probably located at the apical membrane of this cells (Husted et al. 1995; Boese et al. 2004). However, no study has attempted to investigate the nature of the basolateral bicarbonate conductance mentioned above.

When explored, bicarbonate conductances have been shown to be mediated by chloride channels. This is the case of the choroid plexus epithelium, where a not yet identified apical Cl^- channel mediates a HCO_3^- flux (Kibble et al. 1996); similarly, in airway, gallbladder, and pancreatic duct epithelia an apical CFTR Cl^- channel mediates bicarbonate secretion (Illek et al. 1997; Moser et al. 2007; Ishiguro et al. 2009). Hence, it is quite plausible that, at the basolateral membrane of IMCD cells, a not previously described Cl^- channel mediates the observed bicarbonate conductance.

With the aim of determining if a Cl^- conductance exhibiting HCO_3^- conductivity is present at the membranes of IMCD cells in primary culture, we explored the anionic conductance in these cells, using the perforated-patch whole cell clamp technique. We observed a time-dependent outward rectifying anion conductance (I_{ovt}) exhibiting a similar conductivity to HCO_3^- than to Cl^-. Based on its time-dependent activation at positive potentials, on its external DIDS, DPC, furosemide, pH and Ca^{2+} sensitivity (Uchida et al. 1993; Uchida et al. 1995; Waldegger and Jentsch 2000; Uchida and Sasaki 2005), and on the previously reported observation of both voltage-gated chloride channels from the kidney (ClC-K) transcripts and ClC-K protein in IMCD

Correspondence to: Juan J. Bolívar, Departamento de Fisiología, Facultad de Medicina, Universidad Nacional Autónoma de México, Mexico City DF, 04510, Mexico
E-mail: jjboliv@unam.mx
        jumedfis@hotmail.com

(Uchida et al. 1993; Vandewalle et al. 1997; Waldegger et al. 2002) we inferred that this anion conductance could be mediated by ClC-K channels.

Materials and Methods

Cell culture

Wistar rats (175–225 g) were grown and handled in accordance with the guidelines and principles of the Institutional Animal Care Committee of the National Autonomous University of Mexico. Primary cultures of rat IMCD cells were obtained using a modified hypotonic lysis method as described previously (Escobar et al. 2004). Cells were plated on glass cover slips contained in 35 mm Petri culture dishes, and cultured in Dulbecco's modified Eagle medium (DMEM, GIBCO) supplemented with 10% fetal bovine serum (GIBCO), antibiotics and insulin, at 37°C with an air/5% CO_2 atmosphere. Cells were studied 6–11 days after plating. At this time, cells formed confluent cell monolayers exhibiting blister formation, an evidence of cell polarization and transepithelial transport. As described in Escobar et al. (2004), electrophysiological recordings were performed in cells exhibiting principal or IMCD cell morphology (as evidenced by positive *D. biflorus* lectin binding), the main cell population in our cultures.

Whole-cell clamp recordings

Membrane currents were studied with the perforated-patch whole-cell clamp technique, as previously described (Escobar et al. 2004; Bolívar et al. 2008). Coverslips with a confluent-cell monolayer were placed in a superfusion chamber.

In a first group of experiments, cells were maintained in a standard control bath solution containing (in mM): NaCl 45.5, KCl 5, NaH_2PO_4 2.5, Na_2HPO_4 10, calcium citrate 0.4 (1.2 Ca^{2+}), $MgCl_2$ 1, glucose 10, alanine 1, $NaHCO_3$ 17.5, Na-HEPES 54, as well as amiloride 3×10^{-7} M and fenol red 16 mg/l. After equilibration with a mixture of air/5% CO_2 (CO_2 partial pressure (PCO_2), 29.25 mmHg), pH was stabilized at 7.4. Other bath solutions used in this group of experiments were: 1) a "low Cl^-/low HCO_3^- bath solution" containing 1 mM NaCl (8 mM Cl^-), 3 mM $NaHCO_3$ and 113 mM Na-HEPES ; 2) a "low HCO_3^- bath solution" containing 3 mM $NaHCO_3$ and 68.5 mM Na-HEPES (PCO_2 was lowered to ~ 5 mmHg to reach a pH of 7.4); 3) a "low Cl^- bath solution" containing 1 mM NaCl (8 mM Cl^-) and 98.5 mM Na-HEPES; 4) a "high Cl^- bath solution" containing 95.5 mM NaCl (102.5 mM Cl^-) and 4 mM Na-HEPES; and 5) a "high HCO_3^- bath solution" containing 52.5

mM $NaHC_3O$ and 19 mM Na-HEPES (the solution was equilibrated with 15% CO_2 (PCO_2 87.75 mmHg) in order to obtain a pH of 7.4.

In a second group of experiments, cells were initially bathed in the high Cl^- solution described above ("high Cl^- control bath solution), and, thereafter, the PCO_2 of this solution was modified to obtain either a solution with a pH of 7.1 (PCO_2 58.2 mmHg) or a solution with a pH of 7.7 (PCO_2 14.7 mmHg).

In a third group of experiments, phosphates in the high Cl^- control bath solution were replaced by Na-HEPES, and the calcium citrate concentration was modified to obtain either a solution containing 0.5 mM Ca^{2+} or a solution containing 2 mM Ca^{2+}. Cells were initially studied in the 0.5 mM Ca^{2+} solution.

In a fourth group of experiments, cells were initially bathed in a "chloride control (HCO_3^- free, non CO_2 equilibrated) bath solution" containing 113 NaCl (120 mM Cl^-), 5 Na-HEPES; thereafter, 112 mM NaCl in this solution was equimolary replaced by NaBr (bromide solution), NaI (iodide solution) or $NaNO_3$ (nitrate solution).

Osmolarity of every solution was adjusted, with urea, to 300 mOsm/l. All experiments were performed at room temperature (20–25°C). Micropipettes (Kimax-51 glass; Kimble), were filled from the tip with a pipette solution composed of (in mM): KCl 114, NaCl 7.5, NaH_2PO_4 2.5, K_2HPO_4 10, $CaCl_2$ 1.54, $MgCl_2$ 1, glucose 10 and EGTA 2.5; pH 7.4. Pipette filling was completed, from the back, with the same pipette solution containing, in addition, 200 μg/ml amphotericin B. Once filled, micropipettes had a resistance of 2–4 MΩ. Seals were obtained after pipettes had contacted the cell membrane and a gentle suction had been applied. Perforated-patch whole-cell clamp configuration was obtained 4–8 min after the membrane contact, as monitored when a voltage square pulse (20 mV, 5 ms) evoked a capacitive current transient shorter than 3 ms. Membrane potential was clamped at –50 mV. The voltage-clamp protocols were generated and the membrane currents were acquired with the Axopatch-1D under the control of the pClamp software (v.6; Axon Inst.) running on a Pentium 1 PC (Gateway 2000) and using a Digidata 1200 A/D converter (Axon Inst.). Membrane currents were low-pass filtered (at 5 kHz), digitized and stored on the hard disk of the computer for subsequent analysis. Analysis was performed using the Clampfit module of pClamp software, and curve fitting was performed using Sigmaplot (Jandel Scientific). As previously reported (Escobar et al. 2004; Bolívar et al. 1987), the time course of the capacitive current (evoked by a pulse from –50 to –60 mV) exhibited monoexponential decay, evidencing the absence of electrical coupling between cells, an indispensable condition for achieving space clamp. A basic stimulation protocol was used in every cell: from a holding potential of –50 mV,

a series of 720 ms voltage steps between –160 and 80 mV were applied in 20 mV increments and with 8 s intervals between the steps. After each voltage step, membrane potential was fixed at –150 mV during 80 ms, to record the tail currents. The voltage clamp protocols used to determine the slope conductance and the reversal potential, as well as those used to study the tail currents time-dependent kinetics will be described below.

Current kinetics analysis

Depolarization-activated, time-dependent current: it was obtained from currents recorded at membrane potentials between 20 and 80 mV, by subtracting instantaneous current (current values obtained within the first 0.4 ms of voltage pulses).

Instantaneous current: current recorded during the first 0.4 ms of voltage pulses is defined as instantaneous current. Instantaneous current corresponding to voltages steps from –120 to –20 mV was plotted against voltage and instantaneous linear slope conductance was calculated by linear regression. Instantaneous linear current at voltages from 0 to 80 mV was calculated by extrapolation. Cells exhibiting inward rectification (Bolívar et al. 2008) were excluded. Outward rectifying instantaneous current was calculated by subtracting linear current from the current measured at the onset of the voltage pulses from 0 to 80 mV.

Time course of the depolarization-activated outward current: It was studied using instantaneous current-subtracted traces from cells having currents that reach an apparent plateau at the end of the 80 mV pulses. The time course of current activation was fitted with a sum of two exponential functions

$$I_t = A\left\{\left[1 - e^{-\frac{t}{\tau_f}}\right] + \left[1 - e^{-\frac{t}{\tau_s}}\right]\right\} \qquad (1)$$

where I_t is the current measured at time = t, A is a constant related to the maximum value that can be reached by the depolarization-activated and time-dependent current, τ_f and τ_s are the time constants of activation, τ_f being faster than τ_s. In some cells at the more depolarizing potentials, and in every cell at a membrane potential of 20 mV the time-dependent kinetics was fitted with a single exponential function (Eq. 1 without the second exponential term).

Voltage-dependence of the depolarization-activated outward current activation: tail currents (–150 mV) after each voltage step were linear current subtracted. The resultant tail currents (i_v) corresponding to each voltage step (V) were normalized as fractions of the tail current corresponding to the 80 mV step (i_{80}). The normalized values were fitted with the following (Boltzmann type) equation

$$\frac{i_v}{i_{80}\,c} = \frac{i_v}{i_{max}} = \left\{1 + e^{\frac{(V_o - V)}{k}}\right\}^{-1} \qquad (2)$$

where c is a correction factor to account for a non maximal activation of the outward current at 80 mV, i_{max} is the estimated maximum value that can be reached by i_v, V_o is the voltage of half maximal activation, and *k* is a constant which gives the steepness of the voltage dependence.

Tail currents time-dependent kinetics: from a holding potential of –50 mV, the current was activated with a prepulse to 80 mV during 1.1 s, and tail currents were evoked by a series of 880 ms voltage steps between –60 and 60 mV, applied in 20 mV increments and at 16 s intervals. Tail currents, recorded between –60 and –20 mV, were instantaneous currents subtracted and the time course of its deactivation was fitted with Eq. 1.

Voltage ramps, reversal potential and v-ramp response slope conductance: from a holding potential of –50 mV, the current was activated with a prepulse to 80 mV during 1.1 s. Voltage was returned to –60 mV for 3 ms allowing occurrence of capacitative current, and then voltage was ramped to 60 mV over either 30 ms or 7 ms. Time-independent linear current, as measured from recordings obtained with a similar voltage protocol in which a prepulse to –80 mV was applied, was subtracted. The so determined current response to the voltage ramp (current v-ramp response) was plotted against voltage; the reversal potential was measured at the point where the current value crossed the voltage axis, and the slope conductance was determined by linear regression at voltages between ±20 mV of the reversal potential. Three to six prepulse-ramp current responses *per* cell were recorded and, at least, 3 cells *per* experimental condition were studied.
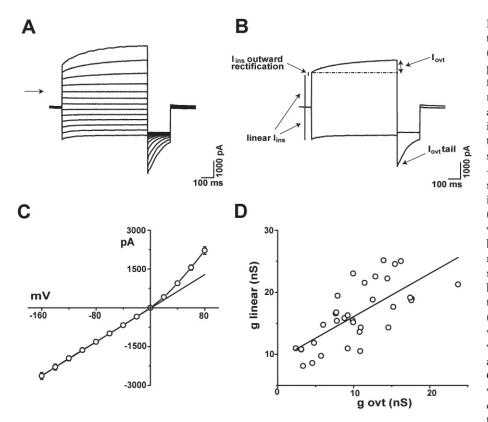
Statistical analysis

All experimental results are expressed as means ± S.E.M. Comparison among mean values was made by Student's *t*-test for paired data. Values of *p* < 0.05 were considered significant.

Results

Time-dependent outward rectifying current and instantaneous linear current

In our previous studies (Escobar et al. 2004; Bolívar et al. 2008), performed in Cl⁻ and HCO₃⁻ free solutions, we described the main cationic currents exhibited by IMCD cells in primary culture. Now we employ Cl⁻ and, usually, HCO₃⁻ containing solutions, to study the main anionic currents present in the membrane of these cells.

A depolarization-activated, time-dependent outward current (I_{ovt}) was observed in about 50% of the studied cells (Figure 1A). It activates at a potential close to 20 mV, requires more than 720 ms to complete its activation at potentials between 20 and 80 mV, and appears to activate more quickly with larger depolarization (see below). Figure 1B illustrates the currents observed in I_{ovt}-expressing cells: an instantaneous current (I_{ins}) exhibiting linear and outward rectifying components and I_{ovt}, whose activation produces prominent tail currents at –150 mV. I_{ins} has a time-dependent deactivation at potentials below –60 mV (Figure 1A, bottom 5 records). A current-voltage (I-V) relationship of the averaged maximal current amplitude of 35 I_{ovt}-expressing cells (selected on the basis of its voltage-dependent activation correction factor, c < 1.3; see Eq. 2 in Materials and Methods) is shown in Figure 1C (circles); note the presence of outward rectification and the zero current potential (E_{0cur}) close to 0 mV (1.1 ± 0.5 mV) of the instantaneous linear current. The outward rectification is mainly due to I_{ovt} (81.3 ± 2.8% at 80 mV). In order to determine whether, in IMCD cells, I_{ins} was related to I_{ovt}, we looked for a correlation between them. Figure 1D

shows a plot of single cell I_{ins} linear slope conductance as a function of the corresponding I_{ovt} chord conductance (determined at 80 mV, assuming an E_{rev} = 10 mV, see below). This plot revealed a significant correlation between the two currents (r = 0.75, slope = 0.69, p < 0.0001, n = 35). This correlation suggests that I_{ovt} channels have a non voltage-dependent activity that contributes to the linear current. A non voltage-dependent activity of I_{ovt} channels is also suggested by the I_{ins} time-dependent deactivation at potentials below –60 mV.

Time-dependent kinetics and voltage dependence of I_{ovt} activation

The time dependence of I_{ovt} activation was studied in those cells that appears to reach an apparent plateau at the 80 mV pulse end (n = 10). In most of these cells, the time course of current activation was well fitted by a sum of two exponential functions (Eq. 1 in Materials and Methods) as shown in Figure 2A. Figure 2B shows a plot of the mean value of τ_f as a function of voltage. All the plotted values exhibit a significant difference between them, indicating that the

Figure 1. Depolarization-activated, time-dependent outward currents (I_{ovt}) in IMCD cells. **A.** Superimposed traces of current recorded from an I_{ovt}-expressing cell. Arrow indicates zero current level and outward currents are upward in this and all subsequent current traces. **B.** Two of the current traces shown in A (those evoked by the –160 and 60 mV voltage steps) are separately shown to illustrate: the instantaneous (I_{ins}) linear current (its amplitude is represented by the vertical bars at left, above and below the base line); the I_{ins} outward rectification (its amplitude corresponds to the single vertical bar at left); the depolarization-activated, time-dependent outward current (I_{ovt}; trace above the dashed line, whose amplitude corresponds to the vertical two heads arrow at right); and the I_{ovt} tail current at –150 mV. **C.** I-V relationship of the mean values (n = 35) of total maximal current (circles); the straight line is the linear fit of I_{ins} extrapolated to the more positive voltage values, to show the outward rectification. When not shown, error bars are smaller than symbols. **D.** Single cell linear I_{ins} slope conductance (g linear) is plotted as a function of the corresponding I_{ovt} chord conductance (g ovt) at 80 mV (both conductances determined in the same group of 35 cells). The straight line shows the linear regression fit to the data.

time dependence of I_{ovt} activation is voltage-dependent. τ_s shows a slight voltage dependence, from 315.1 ± 56.1 ms at 80 mV to 601.9 ± 117.7 ms at 40 mV ($p < 0.04$; $n = 6$; not shown). The voltage dependence of I_{ovt} activation was well described by a Boltzmann type equation (Eq. 2 in Materials and Methods; Figure 2C). The mean values of the activation parameters were V_o = 32.03 ± 1.29 mV, k = 22.60 ± 0.68 mV, and c = 1.12 ± 0.01 ($n = 35$), so that, in the selected cells, within 720 ms at 80 mV the I_{ovt} voltage-dependent activation was about 83% of its full activation.

I_{ovt} v-ramp response and anionic nature of I_{ovt}

Since in our previous studies, performed in the absence of any permeating anion (Escobar et al. 2004; Bolívar et al. 2008), we have never observed the I_{ovt} current, we assumed that this is an anionic current. To test this assumption, we analyzed, under various ionic conditions, the currents flowing during a 30 ms or a 7 ms voltage clamp ramps from –60 to 60 mV (henceforth called v-ramp response) applied 3 ms after a 1.1 s prepulse to either 80 or –80 mV in order to, respectively, activate or not $I_{ovt.}$. The results of these procedures are shown in Figure 3A and B. Figure 3A shows the currents recorded during the prepulses and the ramps, and Figure 3B shows the v-ramp responses recorded when I_{ovt} was activated (trace a) or not (trace b); the subtraction (a – b) corresponds to the I_{ovt} v-ramp response (trace c). To validate the use of these ramps in the study of I_{ovt} conductance properties, we analyzed 880 ms tail currents at membrane potentials between –60 and –20 mV, recorded after a 1.1 s prepulse to 80 mV. Tail currents time-dependent deactivation was well fitted by a sum of two exponential functions (Eq. 1 in Materials and Methods) as shown in Figure 3C. Mean values of τ_f were 174.6 ± 25.0, 225.7 ± 35.5 and 283.9 ± 48.7 ms ($n = 20$) at –60, –40 and –20 mV, respectively. These values are much larger than the 30 ms duration of our longer voltage clamp ramp. The use of these voltage clamp ramps is also validated by the plot shown in Figure 3D. Single cell I_{ovt} slope conductance (as determined from I_{ovt} v-ramp response) is plotted as a function of the corresponding I_{ovt} cord conductance (determined at 80 mV); v-ramps of 30 ms and 7 ms duration were used for this plot. The linear fit obtained (r = 0.93, slope = 0.96, $p < 0.0001$, $n = 107$) corroborates the expected good correlation between both conductance. Hence, 30 ms or 7 ms voltage clamp ramps from –60 to 60 mV are adequate to study the I_{ovt} conductance properties. Figure 3E shows the currents recorded, during the prepulses, in the same cell, at two ionic bath conditions: standard control solution (black traces) and a low Cl$^-$/low HCO$_3^-$ solution (gray traces). I_{ovt}, present in the first condition, was absent, and replaced by a slow deactivating current, in the latter condition. It also shows (dashed line trace) the outward current suppressed by this maneuver, to illustrate the current mediated by I_{ovt}

channels. Figure 3F shows the I_{ovt} v-ramp responses corresponding to the experiment illustrated in E. Note that in the control condition, the I_{ovt} v-ramp response inverts at a potential close to 12 mV (11.8 ± 1.1 mV; $n = 9$); and that in the low Cl$^-$/low HCO$_3^-$ condition, this response has a decreased slope conductance (it decreased from 9.02 ± 0.12 nS to 0.64 ± 0.07 nS; $p < 0.0004$, $n = 9$) and appears to invert
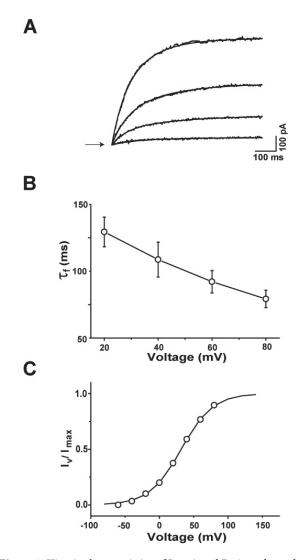

Figure 2. Kinetic characteristics of I_{ovt}. A and B: time-dependent kinetics. **A.** Noisy traces are I_{ins} subtracted currents in response to voltage steps of (from bottom to top): 20, 40, 60 and 80 mV. The lines superimposed to the recordings are the best fits obtained with Eq. 1. I_{ovt} activation becomes faster as depolarizing voltage increases. **B.** Mean values of the fast activation time constant (τ_f; $n = 10$) plotted against the membrane potential, note their voltage dependence. **C.** Voltage-dependent activation. Mean value of the normalized tail currents at –150 mV (I_v/I_{max}; $n = 35$) plotted against membrane potential. The superimposed S-shaped curve corresponds to the best fit obtained with Eq. 2.

close to 60 mV. However, this apparent reversal potential should be taken with caution due to the deactivation of the time-dependent outward current observed during the 80 mV prepulse. Results shown in Figures 3E and 3F indicate that I_{ovt} is an anionic current.

Effect of anionic current blockers on I_{ovt}

Anionic currents may be blocked by external 4,4'-diisothiocyanatostilbene-2,2'-disulfonic acid (DIDS), diphenylaminecarboxylate (DPC) and furosemide (Evans et al. 1986; Schultz et al. 1999; Jentsch et al. 2002; Qu et al. 2003; Uchida and Sasaki 2005), therefore we performed experiments to investigate if I_{ovt} is a DIDS-, DPC- and furosemide-sensitive current. Figure 4A shows the currents recorded, during the prepulses, when the cell was bathed in the standard control solution (black traces), and when this solution contained 1 mM DIDS (gray traces). In the presence of DIDS I_{ovt} amplitude was inhibited by $59.8 \pm 7.2\%$ ($n = 12$, $p < 0.0001$), and I_{ins} was inhibited by $48.5 \pm 3.3\%$ ($n = 12$, $p < 0.0001$); dashed line trace shows the current suppressed by DIDS. Figure 4B shows the I_{ovt} v-ramp
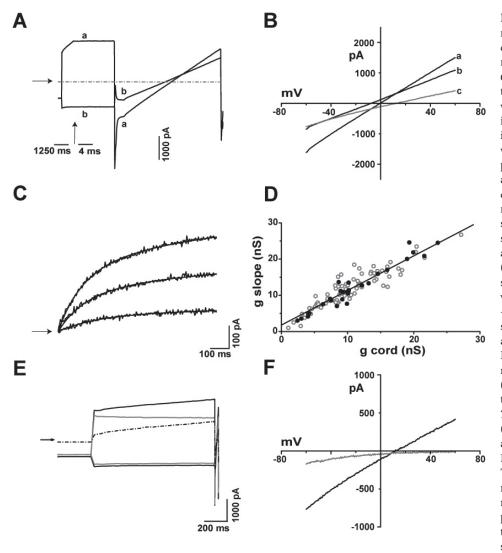

Figure 3. Prepulse I_{ovt} current recordings and I_{ovt} voltage-ramp current responses. **A.** Voltage-ramp (v-ramp; from –60 to 60 mV) current responses obtained when I_{ovt} was activated with a prepulse to 80 mV during 1.1 s (trace a; vertical arrow indicates time scale change) and when it was not activated (prepulse to – 80 mV; trace b). Dash and dot line indicates the zero current level. **B.** v-ramp current traces shown in A, are here separately shown to illustrate the subtraction (a – b), here defined as the I_{ovt} v-ramp response (trace c). **C.** Noisy traces are I_{ins} subtracted I_{ovt} tail currents at voltages of (from bottom to top): –20, –40 and –60 mV. The lines superimposed to the recordings are the best fits obtained with Eq. 1. **D.** Single cell I_{ovt} v-ramp response slope conductance (g slope), as measured with the voltage-ramp protocols of 7 ms (open circles) and 30 ms (closed circles), is plotted as a function of its corresponding I_{ovt} cord conductance (g cord). The straight line shows the linear regression fit to data. **E.** Current recordings obtained during the prepulses (to 80 and –80 mV) in the same cell when bathed in the standard control solution (traces in black) and after this solution were replaced by a low Cl^-/low HCO_3^- solution (traces in gray); note the decrease in outward current amplitude induced by this replacement. The difference between the currents during the prepulse to 80 mV is shown by the dashed line trace to illustrate, in this and subsequent similar figures, the outward current change induced by the experimental maneuver. **F.** I_{ovt} v-ramp responses corresponding to the experiment described in E. Note that, when compared with its control (trace in black), the v-ramp response recorded in the low Cl^-/low HCO_3^- condition (trace in gray) exhibits a decreased slope conductance and a shift in its (extrapolated) reversal potential to a value more positive than 60 mV.

responses corresponding to the experiment illustrated in A. Note that, in the DIDS condition, this response exhibited a decreased slope conductance. I$_{ovt}$ v-ramp response slope conductance decreased from 16.8 ± 1.4 nS, in the control condition, to 4.6 ± 0.6 nS, in the DIDS condition ($n = 12$, $p < 0.0001$), without a change in its reversal potential. On the other hand, Figure 4C shows the currents recorded, during the prepulses, when the cell was bathed in the standard control solution (black traces), and when this solution contained 1 mM DPC (gray traces). In the presence of DPC I$_{ovt}$ amplitude was inhibited by 67.3 ± 5.3% ($n = 12$, $p < 0.0001$), and I$_{ins}$ was inhibited by 45.9 ± 7.9% ($n = 12$, $p < 0.0002$); dashed line trace shows the current suppressed by DPC. Figure 4D shows the I$_{ovt}$ v-ramp re-

sponses corresponding to the experiment illustrated in C. I$_{ovt}$ v-ramp response slope conductance decreased from 5.2 ± 0.3 nS, in the control condition, to 2.0 ± 0.3 nS, in the DPC condition ($n = 12$, $p < 0.0001$), without a change in its reversal potential. Figure 4E shows the currents recorded, during the prepulses, when the cell was bathed in the standard control solution (black traces), and when this solution contained 1 mM furosemide (gray traces). In the presence of furosemide I$_{ovt}$ amplitude was inhibited by 37.3 ± 1.6% ($n = 12$, $p < 0.0001$), and I$_{ins}$ was inhibited by 4.6 ± 0.5% ($p < 0.001$). Figure 4F shows the I$_{ovt}$ v-ramp responses corresponding to the experiment illustrated in E. The addition of furosemide induced a decrease in I$_{ovt}$ v-ramp response slope conductance from 12.6 ± 0.7 nS to
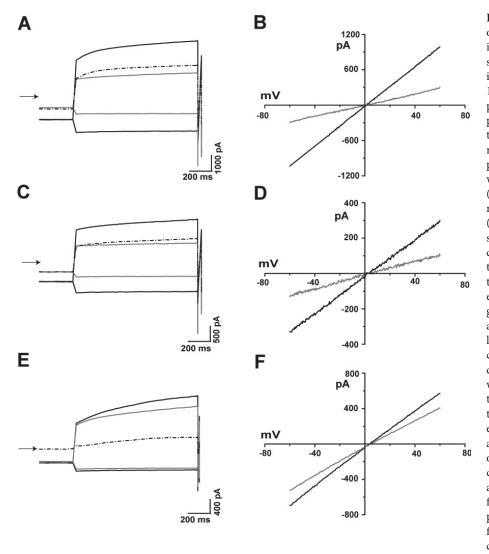

Figure 4. Effect of blocking agents on I$_{ovt}$. **A.** Prepulse current recordings obtained in the same cell in the standard control condition (traces in black), and after its exposure to 1mM DIDS (traces in gray). In the presence of DIDS, I$_{ovt}$ and I$_{ins}$ were partially inhibited, as illustrated by the dashed line trace. **B.** I$_{ovt}$ v-ramp responses corresponding to the experiment described in A. Note that, when compared with its control (trace in black), the v-ramp response recorded in the DIDS condition (trace in gray) exhibits a decreased slope conductance. **C.** Prepulse current recordings obtained in the same cell in the control condition (traces in black), and after its exposure to 1 mM DPC (traces in gray). DPC partially inhibited I$_{ovt}$ and I$_{ins}$, as illustrated by the dashed line trace. **D.** I$_{ovt}$ v-ramp responses corresponding to the experiment described in C. When compared with its control (trace in black), the v-ramp response recorded in the DPC condition (trace in gray) exhibits a decreased slope conductance. **E.** Prepulse current recordings obtained in the same cell in the control condition (traces in black), and after its exposure to 1 mM furosemide (traces in gray). I$_{ovt}$ amplitude decreases in the presence of furosemide. **F.** I$_{ovt}$ v-ramp responses corresponding to the experiment described in E. When compared with its control (trace in black), the v-ramp response recorded in the furosemide condition (trace in gray) exhibits a decreased slope conductance.

8.7 ± 0.4 nS ($n = 12$, $p < 0.0001$), without a change in its reversal potential.

Cl⁻ and HCO₃⁻ conductivity of I_{ovt}

In order to study the relative permeability of I_{ovt} conductance to Cl^- and HCO_3^-, we changed the concentration of these anions, one at a time. For these experiments we used 30 ms v-ramps. When the bath solution Cl^- concentration was reduced from 52.5 mM to 8 mM, the amplitude of I_{ovt} during the prepulse to 80 mV decreased (Figure 5A) from 833.8 ± 63.0 pA in the control condition to 544.8 ± 36.0 pA in the low Cl^- condition ($p < 0.0001$; $n = 23$). Reduction in bath Cl^- concentration induces a decrease in I_{ovt} v-ramp response slope conductance (Figure 5B) from 12.19 ± 0.94 nS to 8.31 ± 0.51 nS ($p < 0.0001$; $n = 23$); and a shift in its reversal potential to a slightly more depolarized value, from 8.13 ± 0.65 mV to 10.22 ± 1.06 mV ($p < 0.001$). Then, I_{ovt} is a Cl^- carrying current. A decrease in I_{ovt} amplitude at 80 mV, from 862.3 ± 52.7 pA to 681.5 ± 48.7 pA ($p < 0.0001$; $n = 24$), was similarly observed when the bath solution HCO_3^- concentration was reduced from 17.5 mM to 3.0 mM (Figure 5C). Bicarbonate reduction also induces a decrease in I_{ovt} v-ramp response

slope conductance (Figure 5D) from 13.09 ± 0.88 nS to 10.64 ± 0.67 nS ($p < 0.0001$; $n = 24$), and a shift in its reversal potential to a slightly more depolarized value, from 7.37 ± 0.51 mV to 8.78 ± 0.64 mV ($p < 0.0001$). Then, I_{ovt} is also a HCO_3^- carrying current. We also explored the expected changes in I_{ovt} amplitude and I_{ovt} v-ramp response when the bath solution permeating anions concentration was increased. A rise in the Cl^- concentration from 52.5 mM to 102.5 mM provokes an increase in the I_{ovt} amplitude (Figure 6A) from 300.8 ± 32.9 pA to 719.2 ± 104.2 pA ($p < 0.0002$; $n = 12$); and, as expected, it also evokes an increase in I_{ovt} v-ramp response slope conductance (Figure 6B), from 6.51 ± 0.73 nS to 13.18 ± 1.78 nS ($p < 0.0001$; $n = 12$); and a shift in its reversal potential to a less depolarized value, from 8.68 ± 0.92 mV to 6.87 ± 0.74 mV ($p < 0.002$). When the HCO_3^- concentration was augmented from 17.5 mM to 52.5 mM, the I_{ovt} amplitude increased (Figure 6C) from 447.8 ± 80.4 pA to 811.4 ± 123.1 pA ($p < 0.0001$; $n = 16$). I_{ovt} v-ramp response slope conductance also increased (Figure 6D) from 8.61 ± 1.48 nS to 13.68 ± 2.46 nS ($p < 0.001$; $n = 16$), and its reversal potential shifted to a less positive value from 8.91 ± 1.48 mV to 5.57 ± 1.30 ($p < 0.0001$). When we express the observed changes in I_{ovt} v-ramp response slope conductance as slope conductance
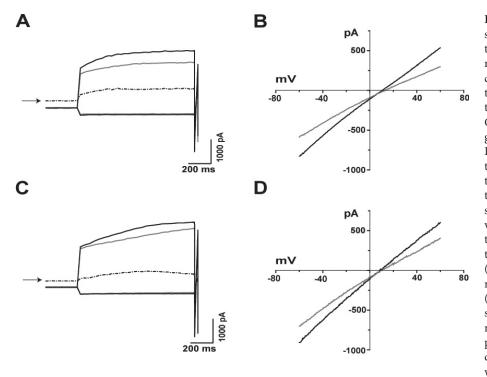

Figure 5. Effect of a decrease in bath solution Cl^- or HCO_3^- concentration on I_{ovt}. **A.** Prepulse current recordings obtained in the same cell in the standard control condition (traces in black), and after this solution was replaced by a low Cl^- concentration solution (traces in gray). Note the decrease in outward I_{ins} and I_{ovt} amplitudes induced by this reduction in bath Cl^- concentration. Dashed line trace illustrates the Cl^- carried outward current suppressed by this maneuver. **B.** I_{ovt} v-ramp responses corresponding to the experiment described in A. Note that, when compared with its control (trace in black), the v-ramp response recorded in the low Cl^- condition (trace in gray) exhibits a decreased slope conductance and a shift in its reversal potential to a slightly more positive value. **C.** Currents recorded during the prepulses in the same cell when bathed in the standard control solution (traces in black) and after this solution was replaced by a low HCO_3^- concentration solution (traces in gray). Reduction in bath HCO_3^- concentration induces a decrease in I_{ovt} amplitude. Dashed line trace illustrates the HCO_3^- carried outward current suppressed by this maneuver. **D.** I_{ovt} v-ramp responses corresponding to the experiment described in C. Note that, when compared with its control (trace in black), the v-ramp response recorded in the low HCO_3^- condition (trace in gray) exhibits a decreased slope conductance.

change *per* mM of permeating anion concentration change, we obtain the following values for Cl^- and HCO_3^- concentration reduction, respectively: 0.09 ± 0.01 nS/mM ($n = 23$) and 0.17 ± 0.02 nS/mM ($n = 24$). On the other hand, for Cl^- and HCO_3^- concentration increments the following values are obtained: 0.13 ± 0.02 nS/mM ($n = 12$) and 0.14 ± 0.03 nS/mM ($n = 16$). All together, these results indicate that I_{ovt} channels exhibit a similar conductivity to HCO_3^- and Cl^-. However, when bath solution anion concentration was modified, the observed changes in I_{ovt} v-ramp response reversal potential were smaller than that expected for an anion selective

conductance. When bath solution anion concentration is modified, if I_{ovt} channels localize at the basolateral membrane equivalent of the cultured cells, tight junctions between cells may hinder and delay the expected intercellular anions concentration changes (Cereijido et al. 1981; Contreras et al. 1989; Gonzalez-Mariscal et al. 1990). This could, at least in part, explain the smaller than expected changes in reversal potential. But, in that case, the tight junction diffusion barrier should attenuate the I_{ovt} v-ramp response slope conductance changes, and this was not the case; furthermore, this diffusion barrier should also restrict the blocking agents access to
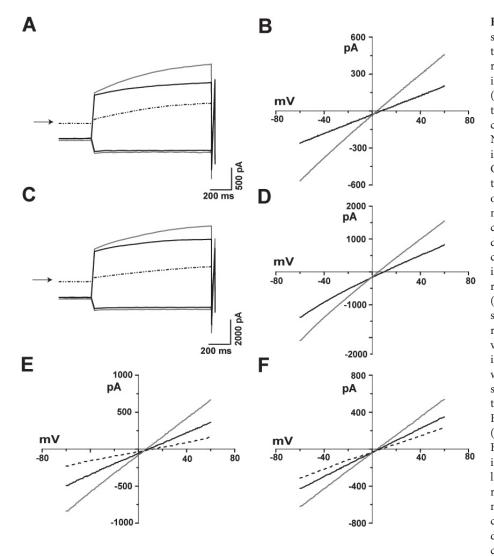

Figure 6. Effect of a change in bath solution Cl^- or HCO_3^- concentration on I_{ovt}. **A.** Prepulse current recordings obtained in the same cell in the standard control condition (traces in black), and after this solution was replaced by a high Cl^- concentration solution (traces in gray). Note the increase in I_{ovt} amplitude induced by this increment in bath Cl^- concentration. Dashed line trace illustrates the Cl^- carried outward current promoted by this maneuver. **B.** I_{ovt} v-ramp responses corresponding to the experiment described in A. Note that, when compared with its control (trace in black), the v-ramp response recorded in the high Cl^- condition (trace in gray) exhibits an increased slope conductance and a shift in its reversal potential to a less positive value. **C.** Currents recorded during the prepulses in the same cell when bathed in the standard control solution (traces in black) and after this solution was replaced by a high HCO_3^- concentration solution (traces in gray). Increment in bath HCO_3^- concentration induces an increase in I_{ovt} amplitude. Dashed line trace illustrates the HCO_3^- carried outward current added by this maneuver. **D.** I_{ovt} v-ramp responses corresponding to the experiment described in C. Note that, when compared with its control (trace in black), the v-ramp response recorded in the high HCO_3^- condition (trace in gray) exhibits an increased slope conductance and a shift in its reversal potential to a less positive value. **E.** I_{ovt} v-ramp responses recorded at three different bath solution Cl^- concentrations: control concentration (52.5 mM Cl^-, solid black trace), high concentration (102.5 mM Cl^-, gray trace) and low concentration (8 mM Cl^-, dashed trace). **F.** I_{ovt} v-ramp responses recorded at three different bath solution HCO_3^- concentrations: control concentration (17.5 mM HCO_3^-, solid black trace), high concentration (52.5 mM HCO_3^-, gray trace) and low concentration (3 mM HCO_3^-, dashed trace). (E and F: I_{ovt} v-ramp responses studied in the tight junction open condition.)

the channels, however, only a several (4–8) minutes delay in blocking agents to attain their maximal inhibitory effect was observed (not shown). Having in mind that, in epithelial cells cultured on impermeable supports, basolateral membrane transport proteins localize mainly at the lateral membrane domain (Moreno et al. 2002; Padilla-Benavidez et al. 2010), we used a condition that favors the opening of tight junctions (Martínez-Palomo et al. 1980), in order to eliminate the possibility that a tight junction diffusion barrier affects our results. Cells were preincubated during 5 min in a Ca^{2+}-free control bath solution plus 2 mM EGTA, and maintained, thereafter, in the no-Ca^{2+} control bath (without EGTA),

until currents from a cell exhibiting I_{ovt} were recorded. Bath was then changed to the standard control bath solution and experiments performed as before, but with the difference that 7 ms v-ramps were employed. Figure 6 (E and F) illustrates the results obtained in this "tight junctions open condition". When bath solution Cl^- concentration was reduced from 55.5 mM to 8 mM, I_{ovt} v-ramp response slope conductance decreased from 7.52 ± 0.50 nS to 3.57 ± 0.32 nS ($n = 18$, $p < 0.0001$) and its reversal potential shifted to a slightly more depolarized value, from 8.44 ± 0.61 mV to 11.50 ± 1.07 mV ($p < 0.0001$); when the Cl^- concentration was increased from 52.5 mM to 102.5 mM the slope conductance increased from
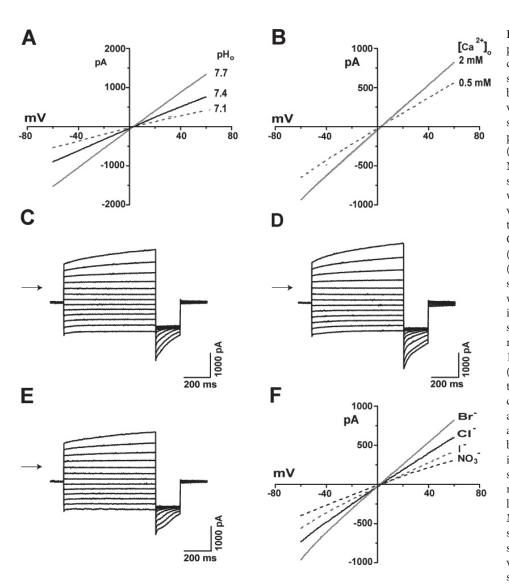

Figure 7. Effects of bath solution pH changes, bath solution Ca^{2+} concentration increase, and bath solution Cl^- partial replacement by Br^-, I^- and NO_3^- on I_{ovt}. **A.** I_{ovt} v-ramp responses recorded in the same cell at three bath solution pH: 7.1 (dashed gray trace), 7.4 (black trace), and 7.7 (gray trace). Note that I_{ovt} v-ramp response slope conductance increased when pH was increased. **B.** I_{ovt} v-ramp responses recorded in the same cell at two bath solution Ca^{2+} concentrations: 0.5 mM (dashed gray trace) and 2 mM (gray trace). I_{ovt} v-ramp response slope conductance increased when Ca^{2+} concentration was increased. **C.** Chloride control solution (120 mM Cl^-). **D.** Bromide solution (8 mM Cl^- and 112 mM Br^-). **E.** Iodide solution (8 mM Cl^- and 112 mM I^-). Note that, when compared with the control chloride condition, I_{ovt} amplitudes and I_{ovt} tail currents amplitudes were larger in the bromide condition and smaller in the iodide condition. (C to E: superimposed traces of currents recorded (using our basic stimulation protocol; see Figure 1A and Materials and Methods) in the same cell at three different bath solution ionic conditions). **F.** I_{ovt} v-ramp responses recorded in the same single cell at the same three conditions as in C to E, and at a nitrate condition (8 mM Cl^- and 112 mM NO_3^-). When compared with its value in the chloride condition (black trace) the v-ramp response recorded in the bromide condition (solid gray trace) exhibits an increased slope conductance; the v-ramp response recorded in the iodide condition (dashed gray trace) exhibits a decreased slope conductance; and that recorded in the nitrate condition (dashed black trace) exhibits an even smaller slope conductance.

6.75 ± 0.47 nS to 12.15 ± 0.40 nS (n = 24, p < 0.0001) and the reversal potential shifted from 8.80 ± 0.47 mV to 6.83 ± 0.31 mV (p < 0.001; Figure 6E). In the same way, when bath solution HCO$_3^-$ concentration was reduced from 17.5 to 3 mM, I$_{ovt}$ v-ramp response slope conductance decreased from 7.38 ± 1.26 nS to 5.45 ± 0.94 nS (n = 24, p < 0.0001) and its reversal potential shifted to a slightly more depolarized value, from 4.78 ± 0.37 mV to 6.27 ± 0.71 mV (p < 0.005), whereas increasing the HCO$_3^-$ concentration from 17.5 to 52.5 mM increased the slope conductance from 5.71 ± 0.70 nS to 8.98 ± 1.37 nS (n = 24, p < 0.0001) and shifted the reversal potential from 6.40 ± 0.52 mV to 5.07 ± 0.33 mV (p < 0.01; Figure 6F). It is clear that results obtained in the tight junctions open condition were similar to those obtained in the usual condition, and therefore we can exclude a role of a tight junction diffusion barrier in our usual experimental condition. Hence, another mechanism must be involved to explain the small changes in I$_{ovt}$ v-ramp response reversal potential observed when bath solution anion concentration was modified. It results, probably, from the presence of an unstirred layer inside the membrane and an I$_{ovt}$ channels non voltage-dependent basal activity (suggested above) allowing a relative fast transmembrane anionic flux, which, in turn, allows the unstirred layer anionic concentrations to change, rapidly, in parallel with bath solution ion concentration modifications. A similar mechanism to explain similar observations has been proposed by others (Palmer and Frindt 2006) when studying a basolateral Cl$^-$ conductance in the isolated cortical collecting duct. For this mechanism to work, and to maintain solutions electrical neutrality, a companion transmembrane cationic flux must occur, probably mediated by the basolateral HCN channels, which exhibit a non voltage-dependent activity (Bolívar et al. 2008).

Is I$_{ovt}$ mediated by ClC-K channels?

At this point, we have identified a Cl$^-$/HCO$_3^-$ conductance, and described the main characteristics of its time- and voltage-dependent activation. Now the question to answer is: what type of Cl$^-$ channels mediates the I$_{ovt}$ current? As mentioned in the introduction, both a CFTR and a CaC Cl$^-$ conductance have been identified in IMCD cells (Husted et al. 1995; Boese et al. 2004). CFTR channels, although permeable to HCO$_3^-$ (Linsdell et al. 1997; Meyer et al. 2000; Shcheynikov et al. 2004), mediate, in IMCD cells, linear, non-outward rectifying currents, that are not sensitive to external DIDS blockade (Husted et al. 1995; Vandorpe et al. 1995). On the other hand, although CaC channels mediate, in IMCD cells, outward rectifying currents (Qu et al. 2003; Boese et al. 2004), they are poorly conductive to HCO$_3^-$ (Qu and Hartzell 2000). Another type of Cl$^-$ channels, the ClC-K channels (ClC-K1 and ClC-K2), has been shown to be present in IMCD cells, at least at the mRNA and protein level (Uchida et al. 1993;

Adachi et al. 1994; Vandewalle et al. 1997; Waldegger et al. 2002). Among the two types of ClC-K channels expressed in rat, ClC-K1 channels mediate DIDS-, DPC- and furosemide-sensitive outward rectifying currents that resemble the I$_{ovt}$ current (Uchida et al 1993, 1995; Uchida and Sasaki 2005). On the other hand, the thin ascending limb of Henle's loop (tALH), a nephron segment expressing ClC-K1 channels (Uchida et al. 1995), exhibits a high HCO$_3^-$ permeability (Flessner and Knepper 1993). Hence, we drive our efforts to test if I$_{ovt}$ is mediated by ClC-K1 channels. Currents mediated by ClC-K channels increase when the external pH or the external Ca^{2+} concentration are augmented, and decrease with the opposite changes (Uchida et al. 1995; Waldegger and Jentsch 2000; Waldegger et al. 2002; Mummery et al. 2005). When we decreased the external pH from 7.4 to 7.1, the I$_{ovt}$ amplitude, during the prepulse to 80 mV, decreased from 805.5 ± 93.0 pA to 426.0 ± 61.2 pA (p < 0.0001; n = 10; not shown), and the I$_{ovt}$ v-ramp response slope conductance decreased from 11.42 ± 1.26 nS to 6.54 ± 0.74 nS (p < 0.0001; n = 10); and when we changed the pH from 7.4 to 7.7, the I$_{ovt}$ amplitude increased from 685.50 ± 102.6 pA to 1265.5 ± 193.9 pA (p < 0.0005; n = 10; not shown), and the I$_{ovt}$ v-ramp response slope conductance increased from 9.89 ± 1.24 nS to 17.99 ± 2.47 nS (p < 0.0002; n = 10). This external pH sensitivity is opposite to that exhibited by CaC channels (Qu and Hartzell 2000). Figure 7A illustrates the changes induced by these pH modifications on the I$_{ovt}$ v-ramp response, whereas Figure 7B shows the change induced on this response by an increase in the external Ca^{2+} concentration. When bath solution Ca^{2+} concentration was raised from 0.5 mM to 2 mM, I$_{ovt}$ amplitude increased from 783.7 ± 17.5 pA to 1211.7 ± 61.6 pA (p < 0.0001; n = 12; not shown); and the I$_{ovt}$ v-ramp response slope conductance increased from 9.84 ± 0.21 nS to 14.73 ± 0.21 nS (p < 0.0001; n = 12). These results support our assumption that I$_{ovt}$ is a current mediated by ClC-K channels.

The anionic conductivity sequence of I$_{ovt}$

ClC-K1 and ClC-K2 channels differ in their anions conductivity ratios (Uchida et al. 1993; Adachi et al. 1994; Waldegger and Jentsch 2000). Therefore, we studied the I$_{ovt}$ current both in a Cl$^-$ rich bath solution (120 mM Cl$^-$) and when 112 mM Cl$^-$ in this solution was equimolar replaced by Br$^-$, I$^-$, or NO$_3^-$. Figure 7(C, D and E) shows the currents recorded, in the same cell, respectively in the chloride-rich, the Br$^-$ and the I$^-$ solution (currents recorded under the NO$_3^-$ condition are not shown); note that, in comparison with the Cl$^-$ control (7C), both I$_{ovt}$ currents and I$_{ovt}$ tail currents were larger in the Br$^-$ condition (7D) and smaller in the I$^-$ condition (7E). Figure 7F illustrates the I$_{ovt}$ v-ramp responses recorded, in the same cell under the four anionic conditions. As measured using the prepulse-ramp voltage protocol, when most Cl$^-$ was replaced by Br$^-$, I$_{ovt}$ amplitude increased from 642.3

± 46.4 pA to 945.5 ± 46.8 pA ($p < 0.0001$, $n = 11$; not shown); the I_{ovt} v-ramp response slope conductance increased from 9.83 ± 0.43 nS to 12.78 ± 0.52 nS ($p < 0.0001$; $n = 11$), and its reversal potential shifted to a slightly less positive value, from 3.68 ± 0.30 mV to 2.92 ± 0.56 mV ($p < 0.0001$). On the other hand, when most Cl^- was replaced by I^-, I_{ovt} amplitude decreased from 755.0 ± 14.6 pA to 557.0 ± 7.5 pA ($p < 0.0001$, $n = 10$; not shown); the I_{ovt} v-ramp response slope conductance decreased from 11.20 ± 0.19 nS to 8.12 ± 0.14 nS ($p < 0.0001$, $n = 10$), and its reversal potential shifted to a slightly more positive value, from 2.22 ± 0.25 mV to 4.53 ± 0.20 mV ($p < 0.0001$); and when most Cl^- was replaced by NO_3^-, I_{ovt} amplitude decreased from 737.2 ± 109.7 pA to 363.1 ± 107.4 pA ($p < 0.0001$, $n = 10$; not shown); the I_{ovt} v-ramp response slope conductance decreased from 11.33 ± 1.57 nS to 6.33 ± 1.43 nS ($p < 0.0001$; $n = 10$), and its reversal potential shifted to a slightly less positive value, from 4.98 ± 0.64 mV to 2.82 ± 0.21 mV ($p < 0.003$). Then, I_{ovt} channels exhibit a $Br^- > Cl^- > I^- > NO_3^-$ conductivity sequence, which is different from that observed in ClC-K1 channels from renal origin ($Br^- > NO_3^- \geq Cl^- > I^-$, Waldegger and Jentsch 2000) or cochlear origin ($Br^- = Cl^- > NO_3^- > I^-$; Ando and Takeuchi 2000), and is also different from that observed in ClC-K2 channels from renal origin ($Br^- > I^- > Cl^-$; Adachi et al. 1994). Hence, our results suggest that I_{ovt} is mediated by a no previously described ClC-K channel exhibiting a similar conductivity to Cl^- than to HCO_3^-.

Discussion

This work focuses on the study of a bicarbonate conductance, observed two decades ago, at the basolateral membrane of IMCD cells (Stanton 1989; Imai and Yoshitomi 1990), which was the only anionic current observed either at the basolateral or the apical membrane. In IMCD cells in primary culture, we find a time-dependent outward rectifying anionic current (I_{ovt}), exhibiting a non voltage-dependent component, and which exhibits a similar conductance to HCO_3^- than to Cl^-. Although the voltage and time dependence of I_{ovt} resemble that observed in the CaC currents, previously described in IMCD cell cultures, these CaC currents are not recorded in the basal condition but require their activation by external ATP, and upon activation, currents decay to the non-activated levels within few minutes (Boese et al. 2000, 2004). We have always recorded I_{ovt} in a basal condition, and current recordings may last 1 h or more. Furthermore, CaC currents exhibit $I^- > Br^- > Cl^-$ conductivity sequence (Boese et al. 2000), and an external pH sensitivity opposite to that observed in I_{ovt} (Qu and Hartzell 2000). Hence, I_{ovt} may not be mediated by CaC channels. I_{ovt} may also not be mediated by CFTR, previously described in cultured IMCD cells, because CFTR currents are time and voltage independent,

and exhibit a $I^- > Br^- > Cl^-$ conductivity sequence (Husted et al. 1995; Vandorpe et al. 1995). On the other hand, while the voltage dependence, time course, as well as the external pH, Ca^{2+}, DIDS, DPC and furosemide sensitivity of I_{ovt} resemble those of the currents mediated by ClC-K1 channels (Uchida et al. 1993, 1995; Waldegger and Jentsch 2000; Uchida and Sasaki 2005), I_{ovt} differs from ClC-K1 currents in its $Br^- > Cl^- > I^- > NO_3^-$ conductivity sequence. However, based on its external pH and Ca^{2+} sensitivity, we propose that I_{ovt} may be mediated by a not previously described ClC-K channel. This proposal is supported by the high degree of homology (>80%) existing between the four most studied types of ClC-K channels (ClC-K1, and -K2, from rat, and -Ka and -Kb, from human; Uchida and Sasaki 2005), and by several studies reporting the expression of a ClC-K gene in the rat IMCD cells. Among these studies there are RT-PCR assays reporting the presence of a ClC-K1 transcript (Uchida et al. 1993; Vandewalle et al. 1997; Waldegger et al. 2002), and of a ClC-K2 transcript (Adachi et al. 1994; Vandewalle et al. 1997), though one of such assays did not observe a ClC-K2 transcript (Waldegger et al. 2002). Furthermore, among three immunocytochemistry studies using a ClC-K antibody, which don't discriminate between ClC-K1 and -K2 proteins, one study observed a ClC-K immunoreactivity in IMCD cells (Vandewalle et al. 1997), but this reactivity was not observed by the two others (Mejia and Wade 2002; Pannabecker et al. 2004). These previous results allows us to postulate, with a reasonable certainty, that IMCD cells express a ClC-K channel protein, which identity remains to be determined, and which probably mediates the I_{ovt} current we observed.

Is the I_{ovt} conductance the basolateral bicarbonate conductance previously observed in the isolated and perfused rat IMCD (Stanton 1989)? Although the several minutes delay observed until blocking agents attained their maximal inhibitory effect on I_{ovt} may be suggestive of a basolateral localization of I_{ovt} channels, this observation is not sufficient to confirm this localization. However, a basolateral I_{ovt} conductance, exhibiting an instantaneous, non voltage-dependent activity, may explain the basolateral membrane depolarization observed, in that previous study, when the external pH and bicarbonate concentration were simultaneously decreased, and may also explain the inhibition of this depolarization by DIDS; the absence of a similar depolarization when the external chloride concentration was decreased, would, however, not be compatible with such an explanation.

If I_{ovt} is a basolateral membrane conductance with a non voltage-dependent activity, what physiological role may it perform? The IMCD of the rat is a major site of urinary acidification (Bengele et al. 1986), this is accomplished by an apical active H^+ secretion and by a basolateral passive Na^+-independent bicarbonate reabsorption, which may be

blocked by disulfonic stilbenes (like DIDS and 4-acetamido-4'-isothiocyanatostilbene-2,2'-disulfonic acid (SITS) (Ulrich and Papavassiliou 1981; Praetorius et al. 2004). The I$_{ovt}$ channels, as a DIDS-sensitive basolateral HCO$_3^-$ conductive pathway may probably participate in this bicarbonate reabsorption. Another probable physiological role of I$_{ovt}$ channels has been suggested by us in a previous report (Bolívar et al. 2008). When the kidney acutely passes from a diuresis state to an antidiuresis state (during the early phase of the antidiuretic state) the Na$^+$ and Cl$^-$ transport activity of the tALH provides the basis for an early increment in inner medullary interstitial Na$^+$ and Cl$^-$ concentration (Knepper et al. 2003; Fenton and Knepper 2007; Layton et al. 2009), and, thereafter, the IMCD cells become exposed to a slowly increasing interstitial hypertonicity. In this condition, an influx of Na$^+$ (mediated by HCN channels; Bolívar et al. 2008) and Cl$^-$/HCO$_3^-$ (mediated by I$_{ovt}$ channels) through the basolateral membrane of IMCD may probably allow a rapid cell-interstitium osmotic equilibration, contributing to endow the IMCD cells with the necessary osmotic force for water reabsorption. Hence, the I$_{ovt}$ conductance may probably participate in the IMCD urine concentrating mechanism.

References

Adachi S., Uchida S., Ito H., Hata M., Hiroe M., Marumo F., Sasaki S. (1994): Two isoforms of a chloride channel predominantly expressed in thick ascending limb of Henle's loop and collecting ducts of rat kidney. J. Biol. Chem. **269,** 17677–17683

Ando M., Takeuchi S. (2000): mRNA encoding ‚ClC-K1, a kidney Cl$^-$ channel' is expressed in marginal cells of the stria vascularis of rat cochlea: its possible contribution to Cl$^-$ currents. Neurosci. Lett. **284,** 171–174
http://dx.doi.org/10.1016/S0304-3940(00)01021-1

Bengele H. H., Schwartz J. H., McNamara E. R., Alexander E. A. (1986): Chronic metabolic acidosis augments acidification along the inner medullary collecting duct. Am. J. Physiol. Renal Physiol. **250,** F690–694

Boese S. H., Glanville M., Aziz O., Gray M. A., Simmons N. L. (2000): Ca^{2+} and cAMP-activated Cl$^-$ conductances mediate Cl$^-$ secretion in a mouse renal inner medullary collecting duct cell line. J. Physiol. **523,** 325–338
http://dx.doi.org/10.1111/j.1469-7793.2000.t01-1-00325.x

Boese S. H., Aziz O., Simmons N. L., Gray M. A. (2004): Kinetics and regulation of a Ca^{2+}-activated Cl$^-$ conductance in mouse renal inner medullary collecting duct cells. Am. J. Physiol. Renal Physiol. **286,** F682–692
http://dx.doi.org/10.1152/ajprenal.00123.2003

Bolívar J. J., Cereijido M. (1987): Voltage and Ca^{2+}-activated K$^+$ channel in cultured epithelial cells (MDCK). J. Membrane Biol. **97,** 43–51
http://dx.doi.org/10.1007/BF01869613

Bolívar J. J, Tapia D., Arenas G., Castañón-Arreola M., Torres H., Galarraga E. (2008): A Hyperpolarization-activated, cyclic nucleotide-gated, (Ih-like) cationic current and HCN genes expression in renal inner medullary collecting duct cells. Am. J. Physiol. Cell Physiol. **294,** C893–906

Cereijido M., Meza I., Martínez-Palomo A. (1981): Occluding junctions in cultured epithelial monolayers. Am. J. Physiol. Cell Physiol. **240,** C96–102

Contreras R. G., Avila G., Gutierez C., Bolívar J. J., González-Mariscal L., Darzon A., Beaty G., Rodriguez-Boulan E., Cereijido M. (1989): Repolarization of Na$^+$-K$^+$ pumps during stablishment of epithelial monolayers. Am. J. Physiol. Cell Physiol. **257,** C896–905

Escobar L. I., Martínez-Téllez J. C., Salas M., Castilla S. A., Carrisoza R., Tapia D., Vázquez M., Bargas J., Bolívar J. J. (2004): A voltage-gated K$^+$ current in renal inner medullary collecting duct cells. Am. J. Physiol. Cell Physiol. **286,** C965–974
http://dx.doi.org/10.1152/ajpcell.00074.2003

Evans M. G., Marty A., Tan Y.P., Trautmann A. (1986): Blockage of Ca-activated Cl conductance by furosemide in rat lacrimal glands. Pflügers Arch. **406,** 65–68
http://dx.doi.org/10.1007/BF00582955

Fenton R. A., Knepper M. A. (2007): Mouse models and the urinary concentration mechanism in the new millennium. Physiol. Rev. **87,** 1083–1112
http://dx.doi.org/10.1152/physrev.00053.2006

Flessner M. F., Knepper M. A. (1993): Ammonium and bicarbonate transport in isolated perfused rodent ascending limbs of the loop of Henle. Am. J. Physiol. Renal Physiol. **264,** F837–844

Gonzalez-Mariscal L., Contreras R. G., Bolívar J. J., Ponce A., Chávez de Ramirez B., Cereijido M. (1990): Role of calcium in tight junctions formation between epithelial cells. Am. J. Physiol. Cell Physiol. **259,** C978–986

Husted R. F., Volk K. A., Sigmund R. D., Stokes J. B. (1995): Anion secretion by the inner medullary collecting duct. Evidence for involvement of the cystic fibrosis transmembrane conductance regulator. J. Clin. Invest. **95,** 644–650
http://dx.doi.org/10.1172/JCI117709

Illek B., Yankaskas J. R., Mathen T. E. (1997): cAMP and genistein stimulate HCO$_3^-$, conductance through CFTR in human airway epithelia. Am. J. Physiol. Lung Cell. Mol. Physiol. **272,** L752–761

Imai M., Yoshitomi K. (1990): Electrophysiological study of inner medullary collecting duct of hamsters. Pflügers Arch. **416,** 180–188
http://dx.doi.org/10.1007/BF00370240

Ishiguro H., Steward M. C., Naruse S., Ko S. B. H., Goto H., Case R. M., Kondo T., Yamamoto A. (2009): CFTR functions as a bicarbonate channel in pancreatic duct cells. J. Gen. Physiol. **133,** 315–326
http://dx.doi.org/10.1085/jgp.200810122

Jentsch T. J., Stein V., Weinreich F., Zdebik A. A. (2002): Molecular structure and physiological function of chloride channels. Physiol. Rev. **82,** 503–568

Kibble J. D., Trezise A. E. O., Brown P. D. (1996): Properties of the cAMP-activated Cl⁻ current in choroid plexus epithelial cells isolated from the rat. J. Physiol. **496,** 69–80

Knepper M. A., Saidel G. M., Hascall V. C., Dwyer T. (2003): Concentration of solutes in the renal inner medulla: interstitial hyaluronan as a mechano-osmotic transducer. Am. J. Physiol. Renal Physiol. **284,** F433–446

Layton A. T., Layton H. E., Dantzler W. H., Pannabecker T. L. (2009): The mammalian urine concentrating mechanism: hypotheses and uncertainties. Physiology **24,** 250–256
http://dx.doi.org/10.1152/physiol.00013.2009

Linsdell P, Tabcharani J. A., Rommens J. M., Hou Y. X., Chang X. B., Tsui L. C., Riordan J. R., Hanrahan J. W. (1997): Permeability of wild-type and mutant cystic fibrosis transmembrane conductance regulator chloride channels to polyatomic anions. J. Gen. Physiol. **110,** 355–364
http://dx.doi.org/10.1085/jgp.110.4.355

Martínez-Palomo A., Meza I., Beaty G., Cereijido M. (1980): Experimental modulation of occluding junctions in a cultured transporting epithelium. J. Cell Biol. **87,** 736–745
http://dx.doi.org/10.1083/jcb.87.3.736

Mejia R., Wade J. N. (2002): Immunomorphometric study of rat renal inner medulla. Am. J. Physiol. Renal Physiol. **282,** F553–557

Meyer G., Garavaglia M. L., Bazzini C., Botta G. (2000): An anion channel in guinea pig gallbladder epithelial cells is highly permeable to HCO₃⁻. Biochem. Biophys. Res. Comm. **276,** 312–320
http://dx.doi.org/10.1006/bbrc.2000.3400

Moreno J., Cruz-Vera L. R., García-Villegas M. R., Cereijido M. (2002): Polarized expression of shaker channels in epithelial cells. J. Membrane Biol. **190,** 175–187
http://dx.doi.org/10.1007/s00232-002-1034-4

Moser A. J., Gangopadhyay A., Bradbury N. A., Peters K. W., Frizzell R. A., Bridges R. J. (2007): Electrogenic bicarbonate secretion by prairie dog gallbladder. Am. J. Physiol. Gastrointest. Liver Physiol. **292,** G1683–1694
http://dx.doi.org/10.1152/ajpgi.00268.2006

Mummery J. L., Killey J., Linsdell P. (2005): Expression of the chloride channel ClC-K in human airway epithelial cells. Can. J. Physiol. Pharmacol. **83,** 1123–1128
http://dx.doi.org/10.1139/y05-112

Padilla-Benavidez T., Roldán M. L., Larre I., Flores-Benitez D., Villegas-Sepúlveda N., Contreras R. G., Cereijido M., Shoshani L. (2010): The polarized distribution of Na⁺, K⁺-ATPase: role of the interaction between β subunits. Mol. Biol. Cell. **21,** 2217–2225
http://dx.doi.org/10.1091/mbc.E10-01-0081

Palmer L. G., Frindt G. (2006): Cl⁻ channels of the distal nephron. Am. J. Physiol. Renal Physiol. **291,** F1157–1168
http://dx.doi.org/10.1152/ajprenal.00496.2005

Pannabecker T. L., Abbot D. E., Danzler W. H. (2004): Three-dimensional functional reconstruction of inner medullary thin limbs of Henle's loop. Am. J. Physiol. Renal Physiol. **286,** F38–45
http://dx.doi.org/10.1152/ajprenal.00285.2003

Praetorius J., Kim Y. H., Bouzinova E. V., Frische S., Rojek A., Aalkjær C., Nielsen S. (2004): NBCn1 is a basolateral Na⁺-

HCO₃⁻ cotransporter in rat kidney inner medullary collecting ducts. Am. J. Physiol. Renal Physiol. **286,** F903–912
http://dx.doi.org/10.1152/ajprenal.00437.2002

Qu Z., Hartzell H. C. (2000): Anion permeation in Ca²⁺-activated Cl⁻ channels. J. Gen. Physiol. **116,** 825–844
http://dx.doi.org/10.1085/jgp.116.6.825

Qu Z., Wei R. W., Hartzell H. C. (2003): Characterization of Ca²⁺-activated Cl⁻ currents in mouse kidney inner medullary collecting duct cells. Am. J. Physiol. Renal Physiol. **285,** F326–335

Shcheynikov N., Kim K. H., Kim K., Dorwart M. R., Ko S. B. H., Goto H., Naruse S., Thomas P. J., Muallem S. (2004): Dynamic control of cystic fibrosis transmembrane conductance regulator Cl⁻/HCO₃⁻ selectivity by external Cl⁻. J. Biol. Chem. **279,** 21857–21865
http://dx.doi.org/10.1074/jbc.M313323200

Schultz B. D., Singh A. K., Devor D. C., Bridges R. J. (1999): Pharmacology of CFTR chloride channel activity. Physiol. Rev. (Supp1.) **79,** S109–144

Stanton B. (1989): Characterization of apical and basolateral membrane conductances of rat inner medullary collecting duct. Am. J. Physiol. Renal Physiol. **256,** F862–868

Uchida S., Sasaki S., Furukawa T., Hiraoka M., Imai T., Hirata Y., Marumo F. (1993): Molecular cloning of a chloride channel that is regulated by dehydration and expressed predominantly in kidney medulla. J. Biol. Chem. **268,** 3821–3824

Uchida S., Sasaki S., Nitta K., Uchida K., Horita S., Nihei H., Marumo F. (1995): Localization and functional characterization of rat kidney-specific chloride channel, ClC-K1. J. Clin. Invest. **95,** 104–113
http://dx.doi.org/10.1172/JCI117626

Uchida S., Sasaki S. (2005): Function of chloride channels in the kidney. Annu. Rev. Physiol. **67,** 759–778
http://dx.doi.org/10.1146/annurev.physiol.67.032003.153547

Ullrich K. J., Papavassiliou F. (1981): Bicarbonate reabsorption in the papillary collecting duct of rats. Pflügers Arch. **389,** 271–275
http://dx.doi.org/10.1007/BF00584789

Vandewalle A., Cluzeaud F., Bens M., Kieferle S., Steinmeyer K., Jentsch T. J. (1997): Localization and induction by dehydration of ClC-K chloride channels in the rat kidney. Am. J. Physiol. Renal Physiol. **272,** F678–688

Vandorpe D., Kizer N., Ciampollilo F., Moyer B., Karlson K., Guggino W. B., Stanton B. A. (1995): CFTR mediates electrogenic chloride secretion in mouse inner medullary collecting duct (mIMCDK2) cells. Am. J. Physiol. Cell Physiol. **269,** C683–689

Waldegger S., Jentsch T. J. (2000): Functional and structural analysis of ClC-K chloride channels involved in renal disease. J. Biol. Chem. **275,** 24527–24533
http://dx.doi.org/10.1074/jbc.M001987200

Waldegger S., Jeck N., Barth P., Peters M., Vitzthum H., Wolff K., Kurtz A., Konrad M., Seyberth H. W. (2002): Barttin increases surface expression and change current properties of ClC-K channels. Pflügers Arch. **444,** 411–418
http://dx.doi.org/10.1007/s00424-002-0819-8